

## DIFFERENT TYPES OF PARAMAGNETIC COMPLEXES AND SIZE MANIFESTATION IN EPR MEASUREMENTS OF SMALL CARBON PARTICLES

SZYMON ŁOŚ, LAURENT DUCLAUX\*, WOJCIECH KEMPIŃSKI

Institute of Molecular Physics Polish Academy of Science, ul. Smoluchowskiego 17, 60-179 Poznań, Poland

\*Université de Savoie, 73376 Le Bourget du Lac Cedex, France

Received June 30, 2010; accepted September 6, 2010; published online November 20, 2010.

Two kinds of microporous activated nanostructured carbons were studied by electron paramagnetic resonance (EPR) spectroscopy. They have different specific surface areas: 1500 m<sup>2</sup>/g (AC I) and 2500 m<sup>2</sup>/g (AC II). It was observed that the EPR spectra shapes and their temperature evolution between 300 K and 4 K were depending on the types of carbon sample. Roomtemperature spectra show dissimilar line-widths  $\Delta B = 0.5$  mT and 1.6 mT for AC I and AC II, respectively. The AC I carbon EPR spectra show: (a) a broadening at the beginning of the cooling process, similar to the EPR behavior of graphite and, subsequently and (b) a quick narrowing below 130 K. For the super-activated carbon (AC II), a monotonic narrowing process is observed on decreasing the temperature. These different behaviors were attributed to the size manifestation of graphenes in both activated carbons.

### INTRODUCTION

Recently, microporous activated carbon (AC) turned out to be of interest for many researchers due to its potential of technical applications for gas adsorption (Bénard P, Chahine R, 2001; Xu W-C, Takahashi K, Matsuo Y, Hattori Y, Kumagai M, Ishiyama S, et al. 2007), pollutant removal (Guo J, Lua AC 2002; Wu F-C, Tseng R-L, Juang R-S, 2005; Donnaperma L, Duclaux L, Gadiou R, Hirn MP, Merli C, Pietrelli L. 2009) and electrochemical double layer capacitors (Azaïs P, Duclaux L, Florian P, Massiot D, Lillo-Rodenas M-A, Linares-Solano A, et al. 2007; Schmitt C, Pröbstle H, Fricke J, 2001). A great attention was focused on super AC of specific surface area (SSA) up to 3000 m<sup>2</sup>/g, as calculated by the Brunauer, Emmett, and Teller (BET) method. Currently, microporous AC materials appear to be of interest due to their nanometric dimensions. From the structural analysis viewpoint AC is a disordered material. Transmission electron microscopy studies (Rouzaud JN, Clinard C, 2002) have shown that AC is a conglomerate of layered graphene planes with diverse interlayer distances as well nanometric in-plane dimensions (Łoś Sz., Duclaux L., Kempieński W., Połomska M. 2010). In this paper the attention is focused on different types of paramagnetic complexes formed by electrons and hetero atoms connected to nano-structured carbon particles and probed by EPR method. It is expected that limiting the carbon particles size lead to many changes in properties in comparison to unconfined graphite sheets. Indeed, the boundary carbon

atoms should contribute a significant number of localized electrons at zigzag shaped-edges (Wakabayashi K, Fujita M, Asjiki H, Sigrist M, 2000; Nakada K, Fujita M, Dresselhaus G, Dresselhaus MS, 1996; Wakabayashi K, Fujita M, Ajiki H, Sigrist M, 1999). These electrons can be responsible for the specific properties of different graphitic carbon materials like those containing nano-sized particles with open edges in AC (Enoki T. 2004). Moreover, the domains size limitation leads to modified phonon spectra and that should affect the relaxation processes probed by EPR spectroscopy.

### EXPERIMENTAL

Two kinds of microporous activated carbon samples: AC I and AC II, were studied. The first one (AC I) was prepared from a phenolic resin precursor by a typical steam activation method. The second one (AC II), of commercial name "Maxisorb", was super-activated from a mixture of petroleum coke and an excess amount of potassium hydroxide (Otake T, Nojima Y, Miyazaki T, 1997). The SSA of the AC I and AC II samples, determined with use of the BET method by nitrogen adsorption, amounted to 1500 m<sup>2</sup>/g and 2500 m<sup>2</sup>/g, respectively (Azaïs P. 2003). In order to eliminate the oxygen surface groups generated by the activation process, the activated carbon samples (AC I and AC II) were annealed in a N<sub>2</sub>/H<sub>2</sub> gas flow at 700°C. Activated carbons (typically 5 g) were heated (50°C/min) under a

N<sub>2</sub> atmosphere (flow: 280mL/min) until they have reached 700°C and thereafter annealed at the latter temperature for 2 h under a reducing gas flow (N<sub>2</sub>/H<sub>2</sub> mixture flow: 40mL/min). The reducing treatment aimed at removing completely the oxygenated surface functionalities was successful, since the element analyses indicate the presence of 0.7 at.% and 0.4 at.% only of oxygen in the treated AC I and AC II, respectively. The samples were characterized by electron paramagnetic resonance (EPR) spectroscopy. The measurements have been carried out in the temperature range between 4.2 K and 300 K using an X-band spectrometer equipped with a helium cryostat. The samples have been outgassed at 450 K under  $3.6 \times 10^{-5}$  mbar vacuum prior to the EPR experiments. The samples average masses amounted to 70 µg. They were stored in an EPR silent tube.

## RESULT AND DISCUSSION

The EPR spectra of every AC material reveals an asymmetric line centered on the spectral splitting factor value  $g = 2.0028 \pm 2 \times 10^{-4}$ . Its shape depends on the microwave power. At low temperature and high power the signal saturates. For graphite-like carbon materials the EPR signal comes from the delocalized  $\pi$  conducting electrons at the surface (Wagoner G (1960). A scattering process (between electrons and phonons or electrons and particles boundary) determines the line shape.

As was previously shown (Łoś Sz., Letellier M, Azaïs P, Duclaux L, 2006 ; Kempniński M, Kempniński W, Śliwińska-Bartkowiak M, 2006), the spectra can be fitted by three Lorentzian components. This deconvolution is revealed on Fig 1.

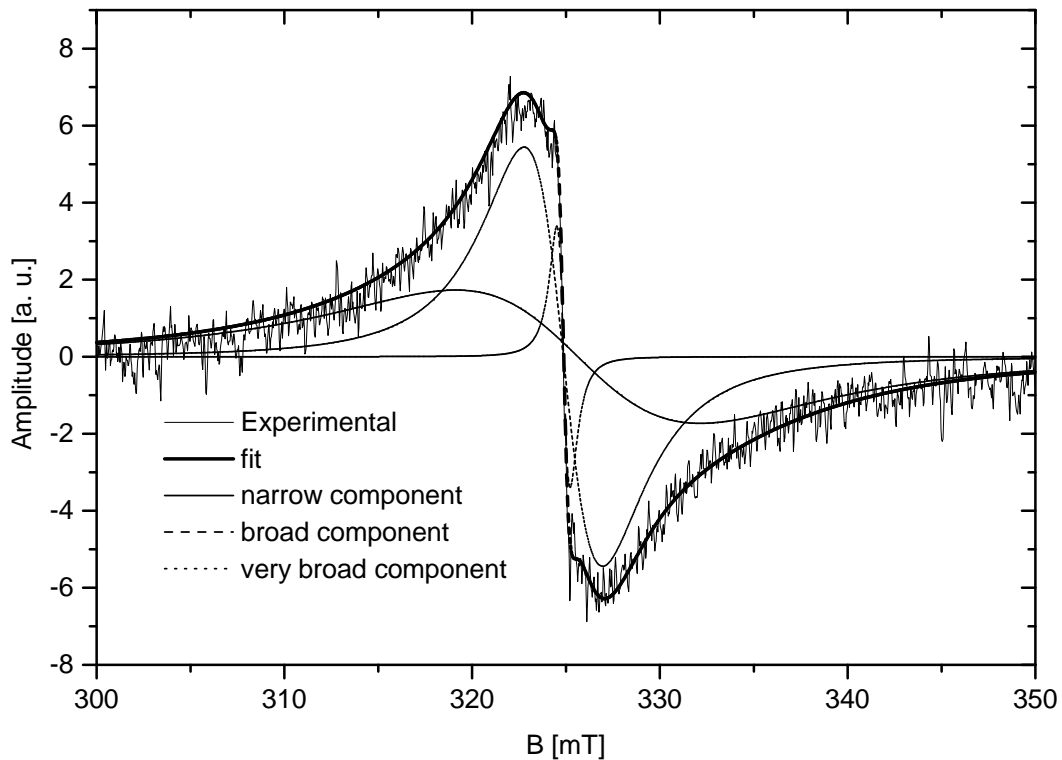


Fig 1. The convolution and fitting result of typical EPR spectra registered at 150 K for AC I.

Each line has a different width and can be described as resulting from different paramagnetic electron states of the carbon particle. The very broad component can be ascribed to the paramagnetic centers created by atoms and molecules interacting with the graphitic surface. These hetero-atoms can be the oxygenated surface

groups formed by activation process or atoms introduced to the carbon structure by an intercalation to obtain a proper stage of graphite intercalation compound. In case of activation process the abundance of surface groups can be controlled by H<sub>2</sub>/N<sub>2</sub> thermal treatment at 700°C described in reference (Azaïs P. 2003). These treatments

result in removing the groups contamination so that the contribution of the very broad component to the paramagnetic susceptibility is decreasing with time of treatment. And contrary, the intercalation process result in increasing of the line intensity with increasing the stage of intercalation. This type of paramagnetic centers are centers with the electrons transfer process in which the whole electron or some fractional part of electron densities are moved between hetero-atoms and carbon atoms system. High abundance of this centers results in strong EPR signal of each components.

Our investigation was focused on a pure carbon system in which after activation process the samples were purified by high temperature treatment and the abundance of very broad component was negligent to the paramagnetic susceptibility. On such prepared samples two other kinds of paramagnetic centers should be taken into careful consideration. They are revealed by broad and narrow components. Such centers have been brought out in a wide class of carbon materials, wherein small particles can be found: carbon black samples (Liu CC, Walters AB, Vannice MA, 1995), ACF (Kempiński M 2006), graphene planes developed from nano-diamonds (Andersson OE, Prasad BLV, Sato H, Enoki T, Hishiyama Y, Kaburagi Y, et al 1998) and also AC (Łoś Sz., 2006; Łoś Sz., 2010). For both kinds of paramagnetic centers located at the graphene planes the  $g$ -value is practically equal. Nevertheless, they are distinguishable by their corresponding line-widths. As the ratio of the line-widths is close to ten, the relaxation time of the localized paramagnetic centers is significantly longer than that of the delocalized ones due to the coupling strength. The evidence for these two different centers was recently found by applying the EPR pulse technique to ACF (Lijewski S, Wanecka M, Hoffmann SK, Kempinski M, Kempinski W, Śliwińska-Bartkowiak M, 2008) where the observed magnetic recovery shows a complex relaxation process in which a slow relaxation is seen on the background of a fast process.

From the point of view of the structure, the AC should be treated as a highly defected material. Nevertheless, in some respects it still resembles graphite. The X-ray investigation shows a strong correlation between the in-plane carbon atoms. This is the reason why one can observe resonances on delocalized  $\pi$  electrons. Taking into account the line-width, the broad component observed in both kinds of samples under consideration can be attributed to this type of paramagnetic center. For example, in thin HOPG (Highly Oriented Pyrolytic Graphite), where the skin depth is negligible, a single Lorentzian line with the  $g$ -value of 2.0031 and a line-

width of 0.5 mT is observed (Stankowski J, Piekara-Sady L, Kempinski W, Huminiecki O, Sczaniecki PB, 1997). Such a width value results from a relaxation mechanism already observed in many carbon materials (Wagoner G., 1960).

Next kind of paramagnetic centers to which the narrow component of EPR spectra is assigned can be localized at the edge of a graphene layer. They are related to the states of polarized electrons in the vicinity of the boundaries of zigzag shape (Wakabayashi K, 2000; Nakada K, 1996; Wakabayashi K., 1999). The presence of boundary states localized on inshore atoms was proposed for the first time on the basis of theoretical calculations and then supported by experimental results with the use of scanning tunneling microscope (Klusek Z, Kozłowski W, Waqar Z, Datta S, Burnell-Gray JS, Makarenko IV, et al., 2005; Klusek Z, Waqar Z, Denisov EA, Kompaniets TN, Makarenko IV., Titkov AN, et al. 2000; Niimi Y, Matsui T, Kambra H, Tagami K, Tsukada M, Fukuyama H, 2005). The narrow component ascribed to these states is caused by a weak coupling between local phonons and in-plane phonons (Igami M, Fujita M, Mizuno S, 1998) giving the longest relaxation time of the third observed component. The proportion of these boundary states, compared to the other ones, is higher in nanostructured carbons. A higher ratio of boundary atoms number with respect to the total number of atoms is observed in materials with finer structures. From EPR spectra recorded at 4.8 K, 8% of the whole amount of the observed spins occupy boundary states in the AC I carbon samples. Taking into account the average in-plane distance between carbon atoms ( $a_c = 0.141$  nm in a graphitic sheet) and the particle dimension of AC I (i.e., 1.7 nm), the ratio of the boundary atoms to the total of atoms is close to 71 at.%. This value is much higher than that corresponding to the observed density of localized states in the EPR spectra (8%). However, supposedly only every fifth boundary atom (or less) can inherit an edge state. The analysis based on the intensity of the narrowest component for the AC II sample has led to similar values of the density of states. A tiny density of localized states was confirmed by the lack of the spin echo in the EPR pulse spectroscopy.

At room temperature, the EPR spectra of purified AC I and AC II reveal line-widths of 0.6 mT and 1.6 mT, respectively. During the cooling process, the line-width of the AC II EPR signal shows a monotonic decrease.

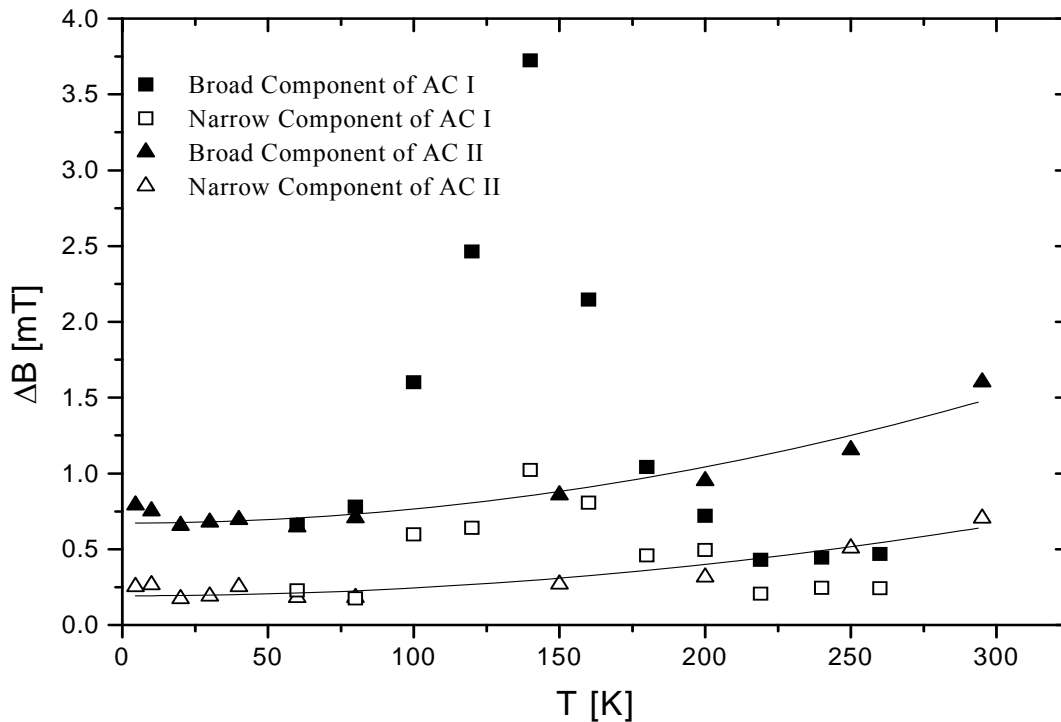


Fig 2. Width of spectra components versus temperature for AC I and AC II samples. Solid lines represents monotone narrowing of AC II components proportional to square of temperature.

The solid lines in Figure 2 represent the quadratic dependences for the narrow and the broad components of the EPR signal from AC II. The line-width of the AC I sample shows a quite different behavior. This line broadens along with lowering the temperature from 300 K to 150 K (line-width increased from 0.5 mT to 3.6 mT). Below 150 K, a sudden narrowing of the EPR line of AC I is observed. It reaches a value comparable to that measured for AC II well below 100 K. The line-width dependence on temperature shows a complex evolution of the spectra. The width of the broad and narrow components of AC I is similar to that of the graphite monocrystal EPR signal (Wagoner G., 1960). Indeed, the HOPG EPR spectra are also broadened on cooling. However, the thermal variations of the spectra for AC I are much stronger here, showing a width ratio close to seven in the range from 130 K to room temperature. As a consequence, EPR spectra were hard to record in a proper way in the temperature range in which the signals are broadened.

As reported in ref. (Wagoner G., 1960), the width of EPR signal can be governed by the scattering of conducting electrons on phonons. Taking into account the analogy between the graphite line and the broad component for AC II, the width of the spectra for AC II can be explained by a metallic relaxation mechanism

(Elliott RJ, 1954; Feher G, Kip AF., 1955). This mechanism requires the assumption that the spectra widths depend on the electric properties. The resistivity of the metal falls off with decreasing temperature. This leads to narrowing of the line-width. Such dependence is observed only for AC II, where the quadratic monotonic narrowing suggests a flipping process (Feher G., Kip A. F., 1955)

The spectra broadening for AC I vs. decreasing temperature displays a rise in relaxation rate due to the growing number of the scattered electrons. As shown by the EPR pulse technique, the excited electron interacts with the carbon lattice causing its deformation. This can be described by two-level tunneling states TLS (Lijewski S., Wanecka M., Hoffmann S. K., Kempinski M., Kempinski W. and Śliwińska-Bartkowiak M., 2008). Such deformations could be localized at the edge of the lattice or are able to propagate through the lattice. At high temperatures, the lattice deformation leads to two characteristic Debye temperatures responsible for longitudinal ( $T_L = 2480$  K) and transverse ( $T_T = 180.5$  K) modes of vibrations (Andersson OE, Prasad BLV, Sato H, Enoki T, Hishiyama Y, Kaburagi Y, 1998). Lowering the temperature results in a change of the phonons spectra. In particular the transverse vibrations are strongly suppressed due to the low value of  $T_T$ . In the

AC case, this attenuation is reinforced by the size effect of small particles imposing a long wavelength limit. Moreover, the exclusion of the transverse mode is expected for a carbon crystallite size lower than critical dimension. Thus, the differences in the behavior of EPR spectra could be brought about by the diversity of the particles lengths. The monotonic narrowing of the EPR signal for AC II presents an evidence for a size unit smaller than the critical one. For AC I, the narrowing process on cooling can be observed well below 130 K because the spontaneous excitation of a transverse mode is excluded by temperature.

### CONCLUSIONS

In our analysis of the EPR spectra we have taken into consideration three different states in which electrons on graphene could be involved. The very broad component of the spectra corresponds to known states created by hetero-atoms interacting with the carbon surface. The broad component is a fingerprint of delocalized  $\pi$  electrons. The narrow component reveals the existence of edge states with abundance increasing with diminishing size of the particle. Due to the low density of localized states, the main part of the EPR signal comes from the delocalized electrons. The line-width is governed by the electron-phonon scattering. For the samples AC II, the observed spectrum is monotonic and narrowing on cooling. This suggests a typical metallic behavior. By contrast, for the AC I samples the spectra broadening is observed at the beginning of the cooling process. This behavior is quite similar to the expansion of graphite spectra on cooling. A sudden spectrum narrowing is observed below 130 K. In fact, the size of the graphene particles imposes limits on phonons in the lower energy level modes. The decreasing temperature attenuates the higher energy modes. This can lead to the exclusion of the transverse phonons vibrations, if the average dimension of the particles is small enough. For the AC II samples, a monotonic spectrum narrowing is observed. However, for larger structural units in the AC I samples the transverse mode starts to be inefficient at 130 K.

### REFERENCES

- Bénard P. and Chahine R. (2001). Determination of the Adsorption Isotherms of Hydrogen on Activated Carbons above the Critical Temperature of the Adsorbate over Wide Temperature and Pressure Ranges *Langmuir*, **17**(6), 1950-1955
- Xu W.-C., Takahashi K., Matsuo Y., Hattori Y., Kumagai M., Ishiyama S., et al. (2007). Investigation of hydrogen storage capacity of various carbon materials *Int J Hydrogen Energy*, **32**(13), 2504-2512
- Guo J. and Lua A. C. (2002). Characterization of adsorbent prepared from oil-palm shell by CO<sub>2</sub> activation for removal of gaseous pollutants *Mater Lett.*, **55**(5), 334-339
- Wu F.-C., Tseng R.-L. and Juang R.-S. (2005). Preparation of highly microporous carbons from fir wood by KOH activation for adsorption of dyes and phenols from water *Separ Purif Tech.*, **47**(1-2), 10-19
- Donnaperna L., Duclaux L., Gadiou R., Hirn M. P., Merli C. and Pietrelli L. (2009). Comparison of adsorption of Remazol Black B and Acidol Red on microporous activated carbon felt. *J Colloid Interface Sci.*, **339**(2), 275-84
- Azaïs P., Duclaux L., Florian P., Massiot D., Lillo-Rodenas M.-A., Linares-Solano A., et al. (2007). Causes of supercapacitors ageing in organic electrolyte *J Power Sourc.*, **171**(2), 1046-1053
- Schmitt C., Pröbstle H. and Fricke J. (2001). Carbon cloth-reinforced and activated aerogel films for supercapacitors *J Non-Cryst Solids*, **285**(1-3), 277-282
- Rouzaud J. N. and Clinard C. (2002). Quantitative high-resolution transmission electron microscopy: a promising tool for carbon materials characterization. *Fuel Processing Techn.*, **78**, 229-235
- Łoś Sz., Duclaux L., Kempniński W. and Połomska M. (2010). Size effect in the characterization of microporous activated nanostructured carbon? *Microporous and Mesoporous Materials*, **130**, 21-25
- Wakabayashi K., Fujita M., Asjiki H. and Sigrist M. (2000). Magnetic properties of nano-graphites at low temperature *Physica B*, **280**(1-4), 388-389
- Nakada K., Fujita M., Dresselhaus G. and Dresselhaus M. S. (1996). Edge state in graphene ribbons: Nanometer size edge shape dependence *Phys Rev B*, **54**(24), 17954-17961
- Wakabayashi K., Fujita M., Ajiki H. and Sigrist M. (1999). Electronic and magnetic properties of nanographite ribbons *Phys Rev B*; **59**(12), 8271-8282.
- Enoki T. (2004). Intercalation and guest-host interaction in nano-graphite *J Phys Chem Solids*; **65**(2-3), 103-108
- Otawa T., Nojima Y. and Miyazaki T. (1997). Development of KOH activated high surface area carbon and its application to drinking water purification *Carbon*, **35**(9), 1315-1319
- Azaïs P. (2003). Recherche des Causes du Vieillessement de Supercondensateurs a Electrolyte Organique à base de carbones actives. PhD thesis. University of Orleans
- Wagoner G. (1960). Spin resonance of charge carriers in graphite *Phys Rev.*; **118**(3), 647-653
- Łoś Sz., Letellier M., Azaïs P. and Duclaux L. (2006). Li doped carbons (activated microporous carbons and graphite): Characterisation by resonance spectroscopies (ESR and <sup>7</sup>Li NMR) and their potentiality for hydrogen adsorption *J Phys Chem Solids*, **67**(5-6), 1182-1185
- Kempniński M., Kempniński W., Śliwińska-Bartkowiak M. (2006). Influence of guest molecules adsorption on electronic properties of activated carbon fibers *Rev Adv Mater Sci.*, **12**(1), 72-77
- Liu C. C., Walters A. B. and Vannice M. A. (1995). Measurement of electrical properties of a carbon black *Carbon*, **33**(12), 1699-1708
- Andersson O. E., Prasad B. L. V., Sato H., Enoki T., Hishiyama Y., Kaburagi Y., et al (1998). Structure and electronic properties of graphite nanoparticles *Phys Rev B*, **58**(24), 16387-16395

- Lijewski S., Wanecka M., Hoffmann S. K., Kempniński M., Kempniński W. and Śliwińska-Bartkowiak M. (2008). Electron spin relaxation and quantum localization in carbon nanoparticle: electron spin echo studies, *Phys Rev B*, **77**, 014304
- Stankowski J., Piekara-Sady L., Kempniński W., Huminiecki O. and Sczaniecki P. B. (1997). EPR of graphite and fullerenes *Fullerene Sci Technol*, **5(6)**, 1203
- Klusek Z., Kozłowski W., Waqar Z., Datta S., Burnell-Gray J. S., Makarenko I. V., et al., (2005). Local electronic edge states of graphene layer deposited on Ir(1 1 1) surface studied by STM/CITS *Appl Surf Sci*, **252(5)**, 1221-1227
- Klusek Z., Waqar Z., Denisov E. A., Kompaniets T. N., Makarenko I. V., Titkov A. N., et al. (2000). Observations of local electron states on the edges of the circular pits on hydrogen-etched graphite surface by scanning tunneling spectroscopy *Appl Surf Sci*; **161(3-4)**, 508-514
- Niimi Y., Matsui T., Kambra H., Tagami K., Tsukada M. and Fukuyama H. (2005). Scanning tunneling microscopy and spectroscopy studies of graphite edges *Appl Surf Sci*; **241(1-2)**, 43-48.
- Igami M., Fujita M. and Mizuno S. (1998). Phonon dispersion of nano-graphite ribbons *Appl Surf Sci*; **130**, 870-875.
- Elliott R. J. (1954). Theory of the effect of spin-orbit coupling on magnetic resonance in some semiconductors *Phys Rev*; **96(2)**, 266-279
- Feher G. and Kip A. F. (1955). Electron spin resonance absorption in metals *Phys Rev*; **98(2)**, 337-348